Center for Turbulence Research
Proceedings of the Summer Program 2014

Numerical scale separation in large-eddy simulation

By R. W. C. P. Verstappen†, W. Rozema†‡ AND H. J. Bae

Large-eddy simulation (LES) seeks to predict the dynamics of spatially filtered turbulent flows. The essence of a scale-separation LES model is that it stops the nonlinear production of smaller scales of motion at the scale set by the filter: there the modeled eddy dissipation has to balance the production. Numerical discretization changes both the nonlinear production and dissipation of sub-filter scales. Therefore, the discrete balance between production and dissipation can deviate from the continuous balance, in particular if a balance is imposed near the scale set by the numerical grid. This paper demonstrates that a scale-separation LES model should attain a production-dissipation balance in the numerical setting. Eddy-viscosity models based on this requirement are derived and successfully applied in simulations of decaying isotropic turbulence and channel flow.

1. Introduction

Most turbulent flows cannot be computed directly from the Navier-Stokes equations, because the range of scales of motion is much too large. Therefore simulations of turbulent flow have to resort to coarse-grained models of the scales for which numerical resolution is not available. In large-eddy simulation (LES) a coarsened description is found by applying a spatial filter to the Navier-Stokes equations. The convective nonlinearity in the Navier-Stokes equations, however, does not commute with a spatial filter. Consequently, an unclosed term is obtained, which represents the effect of the small scales on the larger eddies. When a closure model is introduced, we arrive at

$$\partial_t v + (v \cdot \nabla)v - \nu \Delta v + \nabla p = -\nabla \cdot \tau(v)\,, \tag{1.1}$$

where the closure $\tau(v)$ is to be taken such that the fine details in v are not of interest.

Our research focuses on LES models that can be derived from first principles. The basic idea is that the formation of fine details in the flow should be counterbalanced by the closure model. More precisely, the production of sub-filter scales as a result of the convective nonlinear term in the left-hand side of Eq. (1.1) should be balanced by the sub-filter dissipation resulting from the closure model in the right-hand side. Models that impose this scale-separation condition have been derived (Verstappen *et al.* 2010), but their application in different numerical methods produces mixed results. A scale-separation model was successfully applied in simulations of homogeneous isotropic turbulence with a spectral method (Verstappen *et al.* 2010). However, the same model seems to give insufficient sub-filter dissipation in a simulation of channel flow with a fourth-order accurate finite-volume method (Verstappen 2011).

† Johann Bernoulli Institute for Mathematics and Computer Science, University of Groningen, The Netherlands
‡ Flight Physics & Loads, National Aerospace Laboratory NLR, The Netherlands

This paper demonstrates that the derivation of scale-separation models should take into account the numerics. Because numerical discretization changes both the nonlinear production of sub-filter scales and their dissipation, the balance between production and dissipation can shift, in particular near the scale set by the numerical grid. Therefore a scale-separation model should be derived in a numerical setting: a proper model provides a balance between the discrete (and not the continuous) production and dissipation of sub-filter scales. In this paper discrete scale-separation models are derived. The models are successfully applied in simulations of decaying isotropic turbulence and channel flow with different second-order accurate simulation methods.

2. Scale-separation models for large-eddy simulation

The idea of scale separation can most simply be explained in a continuous setting. To formalize scale separation, we consider a periodic box of turbulence with diameter δ. With the aid of the associated box filter

$$\overline{v} = \frac{1}{|\Omega_\delta|} \int_{\Omega_\delta} v(x,t)\, dx,$$

we can define the sub-filter scales in v by $v' = v - \overline{v}$. The evolution of the $L^2(\Omega_\delta)$ norm of the residual field v' follows from Eq. (1.1)

$$\frac{\mathrm{d}}{\mathrm{dt}} \int_{\Omega_\delta} \tfrac{1}{2}||v'||^2\, dx \;=\; \int_{\Omega_\delta} \left(-\nu||\nabla v'||^2 \;+\; T\left(\overline{v}, v'\right) \;+\; \tau'(v) : \nabla v' \right) dx\,. \tag{2.1}$$

The middle term on the right-hand side is the energy transfer from $\overline{v}$ to v' and the last term is the (negative) eddy dissipation resulting from the closure model $\tau(v)$. Eq. (1.1) does not produce residual scales if the eddy dissipation balances the energy transfer at the scale set by the filter. If the closure model is taken such that the last two terms in Eq. (2.1) cancel, then

$$\frac{\mathrm{d}}{\mathrm{dt}} \int_{\Omega_\delta} \tfrac{1}{2}||v'||^2\, dx \;=\; -\nu \int_{\Omega_\delta} ||\nabla v'||^2\, dx\,, \tag{2.2}$$

and the evolution of the energy of v' does not depend on $\overline{v}$. In other words, the energy of sub-filter scales dissipates at a natural rate without any forcing mechanism involving scales larger than δ. In this way, the scales $< \delta$ are separated from scales $\geq \delta$.

2.1. *Poincaré inequality*

The closure model must keep v' from becoming dynamically significant. The Poincaré inequality

$$\int_{\Omega_\delta} ||v - \overline{v}||^2\, dx \;\leq\; C_\delta \int_{\Omega_\delta} ||\nabla v||^2\, dx \tag{2.3}$$

shows that the $L^2(\Omega_\delta)$ norm of v' is bounded by a constant times the $L^2(\Omega_\delta)$ norm of ∇v. Thus, we can confine the dynamically significant part of the motion to scales $\geq \delta$ by controlling the velocity gradient. The optimal constant C_δ is called the Poincaré constant, and it is the inverse of the smallest non-zero eigenvalue of $-\Delta = \nabla^{\mathrm{T}}\nabla$ on Ω_δ (here the identity $-\nabla\cdot = \nabla^{\mathrm{T}}$ is used). The upper bound given by the Poincaré inequality is sharp, which means that the equality can hold.

To see how the evolution of the $L^2(\Omega_\delta)$ norm of ∇v should be restrained by the closure

model, we consider the residual field v' first. With the help of the Poincaré inequality in Eq. (2.3) and the Gronwall lemma, we obtain from Eq. (2.2) that

$$\int_{\Omega_\delta} ||v'||^2(x,t)\,dx \;\le\; \exp\left(-2\nu t/C_\delta\right) \int_{\Omega_\delta} ||v'||^2(x,0)\,dx\,.$$

In other words, the energy of the residual scales decays at least as fast as $\exp\left(-2\nu t/C_\delta\right)$. The above inequality is sharp. Applying the Poincaré inequality and the Gronwall lemma to

$$\frac{\mathrm{d}}{\mathrm{dt}} \int_{\Omega_\delta} \tfrac{1}{2}||\nabla v||^2\,dx = -\nu \int_{\Omega_\delta} ||\nabla^2 v||^2\,dx \tag{2.4}$$

gives the same rate of decay. Indeed,

$$\int_{\Omega_\delta} ||v'||^2(x,t)\,dx \overset{(2.3)}{\le} C_\delta \int_{\Omega_\delta} ||\nabla v||^2(x,t)\,dx \overset{(2.4)}{\le} C_\delta \exp\left(-2\nu t/C_\delta\right) \int_{\Omega_\delta} ||\nabla v||^2(x,0)\,dx\,.$$

In conclusion, the residual v' can be restrained by imposing Eq. (2.4).

2.2. *Balancing the production of sub-filter scales*

If Eq.(2.4) is satisfied, then the closure model counterbalances the production of scales that are smaller than the box Ω_δ. Rewriting the left-hand side in Eq. (2.4) using Eq. (1.1) and assuming periodicity yields (after integration by parts)

$$\frac{\mathrm{d}}{\mathrm{dt}} \int_{\Omega_\delta} \tfrac{1}{2}||\nabla v||^2\,dx = \int_{\Omega_\delta} \left(-\nu||\Delta v||^2 \;-\; \nabla\left((v\cdot\nabla)v\right) : \nabla v \;-\; \tau(v) : \nabla\,\Delta v \right) dx\,.$$

Thus we see that Eq. (2.4) holds if the contributions of the last two terms on the right-hand side cancel each other out. The middle term on the right-hand side can be expressed in terms of the third invariant

$$r(v) = -\tfrac{1}{3}\mathrm{tr}\left(S^3(v)\right) = -\det\left(S(v)\right)$$

of the rate-of-strain tensor $S(v) = \frac{1}{2}(\nabla v + \nabla v^{\mathrm{T}})$, see for instance (Verstappen *et al.* 2010). Thus we obtain that the energy of the residual scales decays at least as fast as $\exp\left(-2\nu t/C_\delta\right)$ if

$$\int_{\Omega_\delta} \tau(v) : S(\Delta v)\,dx \;=\; 4\int_{\Omega_\delta} r(v)\,dx\,, \tag{2.5}$$

where τ is assumed to be symmetric. In conclusion, the convective contribution to the evolution of the $L^2(\Omega_\delta)$ norm of ∇v is properly balanced by the closure model if Eq. (2.5) holds.

In the above derivation Ω_δ is assumed to be a periodic box. The periodicity conditions are applied to the sub-filter scales in v, not to the full Navier-Stokes solution. In general, homogeneity may be assumed near the smallest scales of motion, which partially justifies the periodicity assumption.

2.3. *The qr eddy-viscosity model*

The most commonly used closure model is given by

$$\tau(v) - \tfrac{1}{3}\mathrm{tr}(\tau)\mathrm{I} \;=\; -2\,\nu_t\,S(v)\,, \tag{2.6}$$

where ν_t denotes the eddy viscosity. The classical Smagorinsky model reads $\nu_t = C_S^2\,\delta^2\sqrt{4q}$ where

$$q(v) = \tfrac{1}{2}\mathrm{tr}(S(v)^2)$$

is the second invariant of the strain rate tensor $S(v)$. For the eddy-viscosity model in Eq. (2.6) the scale-separation condition in Eq. (2.5) reads

$$2\nu_t \int_{\Omega_\delta} S(v) : S(\nabla^{\mathrm{T}}\nabla v)\, dx \;=\; 4 \int_{\Omega_\delta} r(v)\, dx\,, \tag{2.7}$$

where ν_t was assumed to be constant in Ω_δ. The symmetric differential operator $\nabla^{\mathrm{T}}\nabla$ is positive definite on Ω_δ. The Poincaré constant is the inverse of the smallest non-zero eigenvalue of $\nabla^{\mathrm{T}}\nabla$: $0 < 1/C_\delta = \mu_1 < \mu_2 < \ldots$. Hence,

$$\int_{\Omega_\delta} S(v) : S(\nabla^{\mathrm{T}}\nabla v)\, dx \;\geq\; \frac{1}{C_\delta} \int_{\Omega_\delta} S(v) : S(v)\, dx \;=\; \frac{2}{C_\delta} \int_{\Omega_\delta} q(v)\, dx\,,$$

where equality is attained if v is fully aligned with the eigenfunction associated with the smallest eigenvalue $\mu_1 = 1/C_\delta$. Payne & Weinberger (1960) have shown that for convex domains Ω_δ the Poincaré constant is equal to $C_\delta = (\delta/\pi)^2$. Thus, the scale-separation condition is $\nu_t\, \overline{q(v)} \;\geq\; C_\delta\, \overline{r(v)}$, where the bar denotes the box filter over Ω_δ. Taking the minimal amount of positive eddy viscosity gives

$$\tau(v) - \tfrac{1}{3}\mathrm{tr}(\tau)\mathrm{I} \;=\; -2\, C_\delta\, \frac{\max\{0, \overline{r(v)}\}}{\overline{q(v)}}\, S(v)\,. \tag{2.8}$$

This scale-separation eddy-viscosity model will be referred to as the qr model. The qr model has remarkable theoretical properties. For example, its projection on the rate-of-strain tensor is consistent with the leading-order terms of the actual sub-filter tensor (Verstappen 2011). Also, the eddy dissipation of the qr model vanishes at no-slip walls and in flows from Vreman's flow algebra (Vreman 2004). This suggests that taking the minimal eddy viscosity for scale separation adequately describes the sub-filter contributions to the evolution of the filtered velocity.

3. Straightforward discretization of the qr model

In practical implementations of the qr model, the integrals in Eq. (2.8) should be approximated. Use of the midpoint rule gives the approximation

$$\tau(v) - \tfrac{1}{3}\mathrm{tr}(\tau)\mathrm{I} \;=\; -2\, C_\delta\, \frac{\max\{0, r(v)\}}{q(v)}\, S(v)\,. \tag{3.1}$$

The midpoint rule gives a $\mathcal{O}(\delta^3)$ approximation of the ratio of $\overline{r(v)}$ and $\overline{q(v)}$. In this approximation, the ratio of $\overline{r(v)}$ and $\overline{q(v)}$ becomes independent of the box Ω_δ. Thus, it seems that the size of the box enters the discretized model only through the Poincaré constant. A straightforward discretization of the qr model in a spectral method uses the exact Poincaré constant (Verstappen *et al.* 2010)

$$\frac{3}{C_\delta} = \Big(\frac{\pi}{\Delta x}\Big)^2 + \Big(\frac{\pi}{\Delta y}\Big)^2 + \Big(\frac{\pi}{\Delta z}\Big)^2\,. \tag{3.2}$$

In a finite-difference method, a straightforward discretization of the qr model sets the Poincaré constant equal to the inverse of the largest eigenvalue of the discretized diffusion operator $\nabla^{\mathrm{T}}\nabla$ (Verstappen 2011). Thus, a straightforward discretization of the qr model in a second-order accurate method uses the Poincaré constant

$$\frac{1}{C_\delta} = \frac{4}{(\Delta x)^2} + \frac{4}{(\Delta y)^2} + \frac{4}{(\Delta z)^2}\,. \tag{3.3}$$

The straightforward discretization of the qr model in a spectral method gives accurate results for decaying isotropic turbulence (Verstappen *et al.* 2010). However, in this research the straightforward implementation of the qr model in a second-order accurate method was observed to give insufficient eddy dissipation. At first, this was thought to be partially due to the use of the midpoint rule. Therefore, we tried to approximate the actual values of $\overline{r(v)}$ and $\overline{q(v)}$ more accurately using generalized dynamic procedures based on the scale-similarity assumption. The surprising outcome of these investigations is that accurate approximations of $\overline{r(v)}$ and $\overline{q(v)}$ do not consistently improve the performance of the qr model in practice. Instead, it was found that the discretized $\overline{r(v)}$, $\overline{q(v)}$ and the Poincaré constant C_δ should together be proper measures of the numerical production and dissipation of sub-filter scales for the used method. If $\overline{r(v)}$ and $\overline{q(v)}$ are approximated accurately, but the resulting model does not reflect the actual numerical production and dissipation, then scale separation is not attained at the discrete level. This results in simulations with either too little or too much eddy dissipation.

In this paper, we approximate $\overline{r(v)}$ and $\overline{q(v)}$ by the midpoint rule as in Eq. (3.1). The research question then becomes: for what value of the Poincaré constant C_δ does the qr model in Eq. (3.1) attain scale-separation at the discrete level?

4. Proper discretization of scale-separation models

Straightforward discretization of a continuous scale-separation model does not guarantee scale separation at the discrete level. The production-dissipation balance is usually imposed at the scale of a grid cell, and at this scale the numerical production and dissipation can differ considerably from the continuous production and dissipation. Therefore, to attain a proper numerical production-dissipation balance, the order of scale separation and discretization should be reversed. First the governing equations should be discretized, and then the numerical production-dissipation balance should be imposed.

4.1. *The numerical scale-separation condition*

The key to understanding the influence of the numerics on a scale-separation model is to study the effect of the discretized differential operators on the continuous derivation of the scale separation condition. The differential operators in Eq. (1.1) are often implicitly discretized in different ways. In one dimension, for instance, the convective term can be approximated to second-order accuracy as $u_i \left(u_{i+1} - u_{i-1}\right) / \left(2\Delta x\right)$, whereas the diffusive term is approximated as $\left(u_{i+1} - 2u_i + u_{i-1}\right) / \Delta x^2$. Thus, the approximation of the second-order derivative in the diffusion is not equal to the square of the approximation of the derivative that is used for the convective term. Consequently, it is not clear how the invariants of the rate-of-strain and the Poincaré constant of the qr model should be approximated. They are all based on some approximation of ∇, but different approximations of the gradient operator are used for the convective and diffusive term.

To understand how the different discretizations affect the scale separation criterion, we denote the gradient operators in Eq. (1.1) differently. The gradient in the convective term is denoted by ∇_c, the diffusive operator is denoted $-\Delta = \nabla_d^{\mathrm{T}} \nabla_d$, and the right-hand side of Eq (1.1) is $\nabla_d^{\mathrm{T}} \tau$. Furthermore, the gradient in the Poincaré inequality in Eq. (2.3) is denoted by ∇_p. Now, the derivation of the continuous scale-separation condition Eq. (2.5) can be repeated at the discrete level to obtain a numerical scale-separation condition

$$\int_{\Omega_\delta} \tau(v) : S_d(\nabla_p^{\mathrm{T}} \nabla_p v)\, dx \;=\; \int_{\Omega_\delta} \nabla_p \left((v \cdot \nabla_c) v\right) : \nabla_p v \, dx \,. \tag{4.1}$$

In order to express the right-hand side in terms of the third invariant of the discrete rate-of-strain tensor, we have to set $\nabla_p = \nabla_c$. In other words, the gradient from the Poincaré inequality in Eq. (2.3) should be discretized in such a way that $\overline{r(v)}$ is based on the approximation of the derivative in the convective term of Eq. (1.1).

4.2. *Proper discretization of the qr model*

A discrete scale-separation qr model can be derived by substitution of the eddy-viscosity hypothesis $\tau(v) = -2\,\nu_t\,S_d$ in the numerical scale-separation condition in Eq. (4.1) and application of the discrete Poincaré inequality

$$\int_{\Omega_\delta} S_d(v) : S_d(\nabla_p^{\mathrm{T}} \nabla_p v)\,dx \;\geq\; \frac{1}{C_{\delta,p}} \int_{\Omega_\delta} S_d(v) : S_d(v)\,dx \;=\; \frac{2}{C_{\delta,p}} \int_{\Omega_\delta} q_d(v)\,dx\,.$$

This shows that the second invariant $q(v)$ should be discretized using ∇_d, and the Poincaré constant should be equal to the inverse of the largest eigenvalue of $\nabla_p^{\mathrm{T}}\nabla_p = \nabla_c^{\mathrm{T}}\nabla_c$. Taking the minimal eddy viscosity and using the midpoint rule gives

$$\nu_t \;=\; C_{\delta,c}\,\frac{\max\{0, r_c(v)\}}{q_d(v)}\,, \tag{4.2}$$

which corresponds to the discretized qr model

$$\tau(v) - \tfrac{1}{3}\mathrm{tr}(\tau)\mathrm{I} \;=\; -\,2\,C_{\delta,c}\,\frac{\max\{0, r_c(v)\}}{q_d(v)}\;S_d(v)\;. \tag{4.3}$$

Because this model is derived from a numerical scale-separation criterion, the discretizations in the model are determined by the used numerical method.

If the continuous qr model from Eq. (3.1) is discretized straightforwardly, then it seems as if the length scale enters the model only through the Poincaré constant. The above analysis demonstrates that the length scale also enters a discretized model through the discretizations of $\overline{r(v)}$ and $\overline{q(v)}$. Also, the analysis suggests that the Poincaré constant should be set equal to the reciprocal of the largest eigenvalue of the negative Laplacian based on the discretization of the convective derivative $\nabla_c^{\mathrm{T}}\nabla_c$. Thus, for a second-order accurate central discretization $\partial_x u_i = (u_{i+1} - u_{i-1})/(2\Delta x)$, the Poincaré constant should be set in accordance with the decoupled discrete operator $\nabla_c^{\mathrm{T}}\nabla_c$. This gives

$$\frac{1}{C_\delta} = \frac{4}{(2\Delta x)^2} + \frac{4}{(2\Delta y)^2} + \frac{4}{(2\Delta z)^2} = \frac{1}{(\Delta x)^2} + \frac{1}{(\Delta y)^2} + \frac{1}{(\Delta z)^2}\,. \tag{4.4}$$

This Poincaré constant is four times as large as the Poincaré constant used in a straightforward discretization of the qr model. Moreover, if we compare the Poincaré constant with its continuous counterpart $C_\delta = (\delta/\pi)^2$ on a uniform grid $\Delta x = \Delta y = \Delta z$, then it seems that the width of the box filter of the qr model in a second-order accurate central discretization is $\delta = (\pi/\sqrt{3})\,\Delta x$.

The above is a somewhat heuristic derivation of numerical scale-separation models. A thorough derivation of a numerical scale-separation model requires the definition of numerical sub-filter scales, and systematic analysis of their production and dissipation by the numerical method. Nonetheless, the next section shows that proper numerical scale separation is obtained if the Poincaré constant is set according to the suggested procedure.

5. Results

To assess the derived numerical scale-separation condition, the qr model in Eq. (4.3) has been implemented in three kinetic-energy conserving second-order accurate simulation methods: (i) a finite-difference method for low-Mach flow on staggered Cartesian grids, (ii) A finite-volume method for incompressible flow on staggered rectangular grids (Verstappen & Veldman 2003), and (iii) a finite-volume method for compressible flow on collocated curvilinear grids (Kok 2009). In these methods, the eddy viscosity ν_t of the qr model is computed at cell centers. The invariants $r_c(v)$ and $q_d(v)$ are discretized to second-order accuracy. The Poincaré constant is set either to the straightforward discretization in Eq. (3.3), or to the value in Eq. (4.4) suggested by the numerical scale-separation condition.

5.1. *Decaying isotropic turbulence*

In the CTR Summer Program of 2010, it was demonstrated that straightforward implementation of the continuous qr model in a spectral method produces excellent results for decaying isotropic turbulence (Verstappen *et al.* 2010). This suggests that the exact Poincaré constant in Eq. (3.2) gives proper numerical scale separation in a spectral method. For the second-order accurate methods used in this research, the continuous and numerical scale-separation conditions suggest different Poincaré constants. In this section, the effect of the Poincaré constant on numerical scale-separation in second-order accurate simulation methods is investigated by performing simulations of decaying isotropic turbulence.

Simulations of decaying turbulence with the qr model have been performed with the three numerical methods mentioned above. The computational domain is a periodic box of dimensions $2\pi \times 2\pi \times 2\pi$ and the computational grid is uniform with 64 cells in each direction. An initial condition of turbulent flow is generated using the procedure proposed by Kwak *et al.* (1975). The qr model describes the dynamics of a filtered velocity field $v \approx \overline{u}$. Therefore, the initial condition is filtered and results obtained with the qr model are compared with results of a filtered direct numerical simulation (DNS). The resolved velocity field is non-dimensionalized by the square-root of the total kinetic energy of the filtered initial condition. The Reynolds number based on the length of the domain is set to $10,986$ and the dimensionless time step size is set to $\Delta t = 9.2 \times 10^{-2}$.

Figure 1 shows results obtained with the low-Mach method. The results of the qr models are compared with the dynamic Smagorinksy model (Lilly 1992) and a filtered DNS. Although the straightforward discretization of the qr model produces excellent results in a spectral method, it fails in a second-order accurate method. The initial decay rate predicted by the straightforward discretization of the qr model is considerably smaller than the actual decay rate. Also the energy spectrum shows pile-up of kinetic energy near the grid cut-off, indicating that scale separation is not attained at the discrete level. The qr model derived from the numerical scale-separation condition gives better results. Its initial decay rate is in close agreement with the DNS, and no pile-up is observed in the energy spectrum. In fact, results obtained with the numerical qr model collapse on results obtained with the dynamic Smagorinsky model.

The observed behavior is not exclusive to simulations on staggered computational grids. In simulations with the collocated compressible method at $M = 0.1$, the straightforward discretization of the qr model gives insufficient dissipation, whereas the qr model with the numerical Poincaré constant produces good results.

The above results demonstrate that straightforward implementation of a continuous

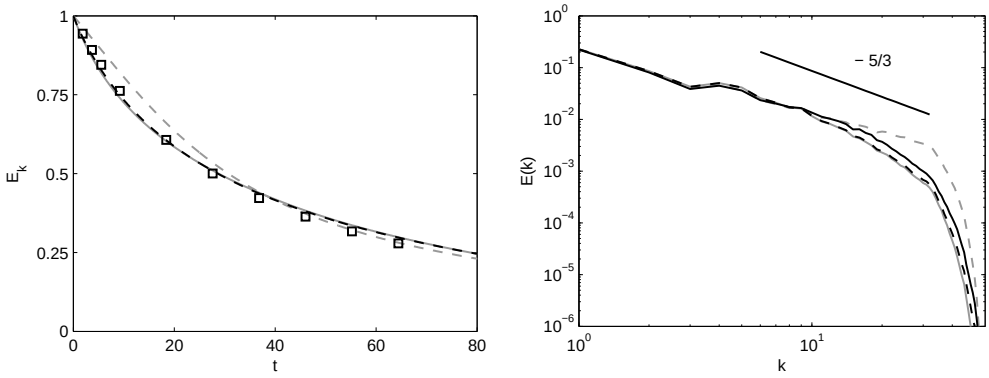

FIGURE 1. The total energy and the energy spectra at time 18.4 in large-eddy simulations of decaying isotropic turbulence with the proper (– –) and straightforward (– –) discretization of the qr model, and with the dynamic Smagorinsky model (——). Also results of a filtered DNS are shown (□ , ——).

scale-separation model does not guarantee scale separation at the discrete level. Numerical scale separation is only attained if the numerical scale-separation condition is satisfied. Therefore, in a second-order accurate method the qr model should use the Poincaré constant given in Eq. (4.4), and not the Poincaré constant suggested by the continuous scale-separation condition.

5.1.1. *The difference between scale separation and the dynamic procedure*

The close agreement of the numerical qr model and the dynamic Smagorinsky model in simulations of decaying isotropic turbulence is remarkable. Close agreement was also observed in similar simulations with a spectral method (Verstappen *et al.* 2010). This seems to suggest that the scale-truncation condition is actually a dynamic procedure in disguise. It is not. Scale-separation models and dynamic models are both derived from first principles, but their modelling assumptions are fundamentally different. The scale-separation condition imposes a balance of production and dissipation of sub-filter scales at a given length scale. The dynamic procedure imposes scale-similarity of the eddy dissipation at two different length scales.

To demonstrate the difference between scale-separation and dynamic models, the simulations from the previous section are repeated with a non-physical initial condition. An initial condition with energy content $E(k) \sim k^{-3/5}$ (instead of $k^{-5/3}$) is generated, and the initial condition is not properly filtered. Figure 2 shows the results of large-eddy simulations without molecular viscosity. For this non-physical flow, the qr model and the dynamic Smagorinsky model give different results. The differences in the energy spectra accurately reflect the assumptions of the both models. The scale-separation model simply truncates the dynamics at the grid cut-off, whereas the dynamic model imposes scale similarity and the corresponding $E(k) \sim k^{-5/3}$ behavior.

5.2. *Turbulent channel flow*

In a previous attempt to simulate channel flow with a straightforward discretization of the qr model in a fourth-order accurate method, the eddy dissipation delivered by the model seemed insufficient (Verstappen 2011). This raises the question whether better results are obtained if the Poincaré constant is set according to the numerical scale-separation condition. To address this question, simulations of turbulent channel flow have been

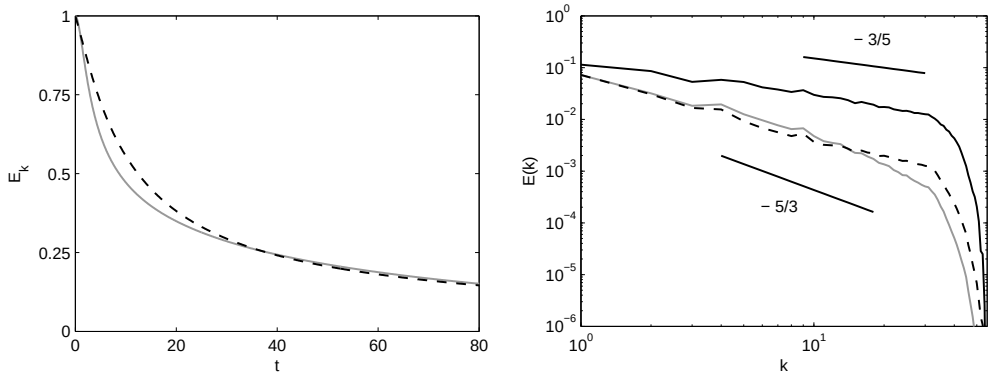

FIGURE 2. The total energy and the energy spectra at time 46.0 in simulations of non-physical flow with the numerical qr model (– –) and the dynamic Smagorinsky model (——). Also the energy spectrum of the initial condition is shown (——).

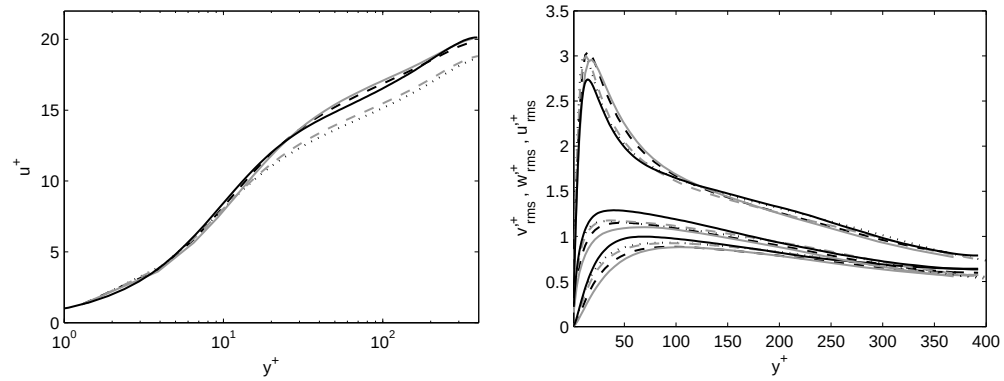

FIGURE 3. Mean velocity profiles and turbulent fluctuations obtained in large-eddy simulations of channel flow without model (· · ·), with the qr model with proper (– –) and straightforward (– –) discretization, and with the Vreman model (——). Also the results of a DNS are shown (——).

performed with the second-order accurate staggered incompressible method. The bulk Reynolds number is set to $\mathrm{Re}_b = 6,875$, which corresponds to a friction Reynolds number $\mathrm{Re}_\tau \approx 395$. The size of the computational domain is $2\pi H \times 2H \times \pi H$ and the grid has 64 cells in each direction. Once again, the qr model is applied both with the straightforward Poincaré constant in Eq. (3.3), and with the numerical scale-separation Poincaré constant in Eq. (4.4). Results obtained with the qr model are compared with results of simulations without a model, with the Vreman model (Vreman 2004), and with results of the direct numerical simulation (DNS) by Moser *et al.* (1999).

Figure 3 shows the mean flow velocity and the turbulent fluctuations normalized by the computed wall friction. The qr model which is based on the continuous scale-separation condition predicts a friction Reynolds number of 416.9. This significantly exceeds the value predicted by a DNS ($\mathrm{Re}_\tau = 392.2$). However, the qr model that satisfies the numerical scale-separation condition predicts a friction Reynolds number of 392.4, in close agreement with both the DNS and the Vreman model ($\mathrm{Re}_\tau = 388.7$).

Just as in simulations of decaying isotropic turbulence, straightforward implementation of a continuous scale-separation model in a second-order accurate method appears to

provide insufficient eddy dissipation in a channel flow simulation. However, a qr model derived from the numerical scale-separation condition gives sufficient eddy dissipation, and for this channel flow it performs as well as the Vreman model.

6. Conclusion

This paper demonstrates that LES models derived from a scale-separation condition should be discretized with care. It was shown that straightforward implementation of a continuous scale-separation model does not guarantee scale separation at the discrete level. Analysis of the discrete production-dissipation balance produced a new numerical scale-separation condition. An eddy-viscosity model that satisfies the numerical scale-separation condition was derived. The derived model produces excellent results in simulations of decaying isotropic turbulence and turbulent channel flow with a second-order method.

Acknowledgments

The authors kindly acknowledge Guillaume Balarac and Antoine Vollant for performing spectral simulations with the qr model during the Summer Program.

REFERENCES

Kok, J. C. 2009 A high-order low-dispersion symmetry-preserving finite-volume method for compressible flow on curvilinear grids. *J. Comput. Phys.* **228**, 6811–6832.

Kwak, D., Reynolds, W. C. & Ferziger, J. H. 1975 *Three-dimensional time dependent computation of turbulent flow.* Technical Report, Stanford University.

Lilly, D. K. 1992 A proposed modification of the Germano subgrid scale closure method. *Phys. Fluids* **4**, 633–635.

Moser, R. D., Kim, J. & Mansour, N. N. 1999 Direct numerical simulation of turbulent channel flow up to $\mathrm{Re}_\tau = 590$. *Phys. Fluids* **11**, 943–945.

Payne, L. & Weinberger, H. F. 1960 An optimal Poincaré inequality for convex domains. *Arch. Ration. Mech. An.* **5**, 286–292.

Verstappen, R. 2011 When does eddy viscosity damp subfilter scales sufficiently? *J. Sci. Comput.* **49**, 94–110.

Verstappen, R. W. C. P., Bose, S. T., Lee, J., Choi, H. & Moin, P. 2010 A dynamic eddy-viscosity model based on the invariants of the rate-of-strain. *Proceedings of the Summer Program*, Center for Turbulence Research, Stanford University, pp. 183–192.

Verstappen, R. W. C. P. & Veldman, A. E. P. 2003 Symmetry-preserving discretization of turbulent flow. *J. Comput. Phys.* **187**, 343–368.

Vreman, A. W. 2004 An eddy-viscosity subgrid-scale model for turbulent shear flow: Algebraic theory and applications. *Phys. Fluids* **16**, 3670–3681.